

# Antiepileptic Teratogen Valproic Acid (VPA) Modulates Organisation and Dynamics of the Actin Cytoskeleton

Peter S. Walmod,\* Galina Skladchikova, Anna Kawa, Vladimir Berezin, and Elisabeth Bock

*Protein Laboratory, Institute of Molecular Pathology, University of Copenhagen, Panum Institute, Copenhagen, Denmark*

The antiepileptic drug valproic acid (VPA) and teratogenic VPA analogues have been demonstrated to inhibit cell motility and affect cell morphology. We here show that disruption of microtubules or of microfilaments by exposure to nocodazole or cytochalasin D had different effects on morphology of control cells and cells treated with VPA, indicating that VPA affected the cytoskeletal determinants of cell morphology. Furthermore, VPA treatment induced an increase of F-actin, and of FAK, paxillin, vinculin, and phosphotyrosine in focal adhesion complexes. These changes were accompanied by increased adhesion of VPA-treated cells to the extracellular matrix. Treatment with an RGD-containing peptide reducing integrin binding to components of the extracellular matrix partially reverted the motility inhibition induced by VPA, indicating that altered adhesion contributed to, but was not the sole reason for the VPA mediated inhibition of motility. In addition it is shown that the actomyosin cytoskeleton of VPA-treated cells was capable of contraction upon exposure to ATP, indicating that the reduced motility of VPA-treated cells was not caused by an inhibition of actomyosin contraction. On the other hand, VPA caused a redistribution of the actin severing protein gelsolin, and left the cells unable to respond to treatment with a gelsolin-peptide known to reduce the amount of gelsolin bound to phosphatidylinositol bisphosphate (PIP<sub>2</sub>), leaving a larger amount of the protein in a potential actin binding state. These findings indicate that VPA affects cell morphology and motility through interference with the dynamics of the actin cytoskeleton. *Cell Motil. Cytoskeleton* 42:241–255, 1999. © 1999 Wiley-Liss, Inc.

**Key words:** cell motility; cell morphology; cytochalasin D; fibroblast; focal adhesions; gelsolin; L-cells; nocodazole; RGD

## INTRODUCTION

The ability of eukaryotic cells to migrate is of fundamental importance in many biological phenomena including embryogenesis, wound healing, immunological responses, and the invasive and metastatic behavior of cancer cells [Van Roy and Mareel, 1992; Bronner-Fraser, 1993; Hauenberger et al., 1997; McCawley et al., 1997].

The magnitude of displacement of a motile cell has been shown in part to depend on cell-substratum interactions [Gail and Boone, 1972; Palecek et al., 1997], maximal cellular dispersion being observed at an intermediate attachment strength.

Contract grant sponsor: Danish Cancer Society; Contract grant sponsor: The Danish Biotechnology Programme; Contract grant sponsor: The EU-Programme on In Vitro Developmental Toxicology; Contract grant sponsor: The Danish Natural Science Council; Contract grant sponsor: The Lundbeck Foundation; Contract grant sponsor: The John and Birthe Meyer Foundation.

\*Correspondence to: Peter S. Walmod, Protein Laboratory, Institute of Molecular Pathology, University of Copenhagen, Panum Institute, Blegdamsvej 3C, Bld. 6.2, DK-2200 Copenhagen N, Denmark.  
E-mail: psw@plab.ku.dk

Received 23 October 1998; accepted 10 December 1998

Another determinant of cell motility is the organisation and function of components of the cytoskeleton. Thus, the amount of various actin isoforms as well as of proteins involved in the organisation and dynamics of the actin cytoskeleton (e.g. vinculin and gelsolin) have been shown to modulate cell motility [Cunningham et al., 1991; Goldmann et al., 1995; Rønnov-Jessen and Petersen, 1996; Kislauskis et al., 1997].

Cellular adhesion and organisation of cytoskeletal components have also been shown to be major regulators of cellular morphology [Willingham et al., 1977; Domnina et al., 1985]. Furthermore, mechanical tension generated within the cytoskeleton, and transmitted to the exterior via cell-cell and cell-extracellular matrix (ECM) interactions have been demonstrated to affect cellular morphology, motility and morphogenesis [Albrecht-Buehler, 1987; Gordon and Brodland, 1987; Ingber et al., 1994].

Valproic acid (2-*n*-propyl pentanoic acid, VPA) is a widely used antiepileptic drug [Mattson, 1995] that also has been shown to be useful in the treatment of manic-depressive illness and migraine [Bowden et al., 1994; Sørensen, 1988]. Besides its anticonvulsive and sedative effects VPA is a known human teratogen causing neural tube defects, spina bifida aperta and anencephaly in 1–2% of human foetuses exposed to the compound during early pregnancy [Robert, 1988]. The molecular mechanisms underlying the teratogenic effects of VPA have not been identified, but a number of VPA analogues having almost identical anticonvulsive, but varying teratogenic potencies have been produced [Fisher et al., 1994; Andrews et al., 1995, 1997].

We have previously been able to demonstrate that the teratogenic potency of VPA and VPA analogues correlates directly with the area and inversely with the motility of cells grown in the presence of these compounds [Berezin et al., 1996; Walmod et al., 1998]. VPA has also been shown to increase the adhesion of C6 glioma cells [Maguire and Regan, 1991; Martin et al., 1988] and to cause alterations in the actin cytoskeleton and focal adhesions of fibroblastoid L-cells [Berezin et al., 1997].

In this study we investigated the effects of VPA on the cytoskeleton of fibroblastoid L-cells in order to elucidate the observed changes in morphology and motility of cells treated with VPA. We show that long-term exposure to VPA stimulated actin stress-fibre formation, and caused an increase in the concentration of F-actin, as well as an increase in focal adhesion formation and cell-substratum adhesion. Although decreasing the cell-substratum adhesion of VPA-treated cells by exposure to an RGD-containing peptide caused a significant increase in cell motility, this treatment could not bring the motility of VPA-treated cells to the level of control cells. The actomyosin cytoskeleton in VPA-treated cells as well as

in control cells was capable of contraction. However, VPA treatment caused a redistribution of the actin-severing protein gelsolin, and in contrast to control cells, the severing activity of gelsolin in VPA-treated cells could not be modulated by a peptide containing one of the PIP<sub>2</sub>-binding domains of gelsolin. These findings indicate that the altered morphology and motility of VPA-treated cells, and thereby the teratogenic effect of the drug, in part may be explained by alterations in the regulation of actin dynamics.

## MATERIALS AND METHODS

### Cell Culture

The L929 cell line was obtained from the European Collection of Animal Cell culture. Clone LVN101 was obtained by transfection of L929 with an empty vector as previously described [Gunning et al., 1987; Meyer et al., 1995].

Cells were grown in Dulbecco's modified Eagle's medium (DMEM) supplemented with 10% (v/v) heat inactivated foetal calf serum, fungizone (2.5 µg/ml), penicillin (100 U/ml) and streptomycin (100 µg/ml) (Gibco BRL, Gaithersburg, MD). Cells were maintained at 37°C in a humidified atmosphere of 5% CO<sub>2</sub>, and had been passaged at least four times and no more than 15 times when used for analysis.

### Chemicals

Sodium-valproate, nocodazole and cytochalasin D were purchased from Sigma (St. Louis, MO). Valproic acid was supplied by Dr. Heinz Nau (School of Veterinary Medicine, Department of Food Toxicology, Hannover, Germany). The integrin binding peptide GRGDSP and the peptide QRLFQVKGR, containing one of the two PIP<sub>2</sub>-binding motifs of gelsolin (residue 161–172) were supplied by the Shemyakin-Ovchinnikov Institute of Bioorganic Chemistry, Russian Academy of Sciences, Moscow.

### Treatment of Cells for Evaluation of Cell Motility and Morphology

Subconfluent cultures were dislodged with 0.5 mg/ml trypsin, 0.54 mM EDTA in a modified Puck's saline (Gibco BRL), seeded in six-well tissue culture plates (Nunc, Roskilde, Denmark) at a density of 1.0–2.0 × 10<sup>3</sup> cells/cm<sup>2</sup>, and grown for 48 h in medium containing 25 mM HEPES.

Cells were exposed to VPA for various times by adding the compound to the medium to a final concentration of 3 mM. 3 M stock solutions of valproic acid or sodium-valproate were dissolved in DMSO and PBS, respectively. Accordingly, control cells were exposed to an equal amount of either DMSO or PBS. In experiments involving the addition of DMSO, the final concentration

of DMSO was always 0.1% (v/v). Experiments performed in the presence of either of the two forms of the drug yielded identical results.

For experiments involving the use of cytochalasin D (1 µg/ml), nocodazole (10 µg/ml), the RGD-peptide (100 and 500 µg/ml), or the gelsolin-peptide (50 µg/ml), the compounds were added to the cell cultures 50 min before cells were fixed for immunofluorescence stainings or recordings were initiated.

### Video Recordings of Live Cells

Video-recordings were done as previously described [Walmod et al., 1998]. Briefly, tissue culture dishes were placed on a motorised, thermostatically controlled heating stage (Lincam Scientific Instruments LTD, Surrey, UK) mounted on a Nikon Diaphot 300 inverted microscope equipped with phase contrast optics and a modified plexiglas incubator (Nikon, Yokohama, Japan) surrounding the microscopic stage. Recordings were obtained using a CCD video camera (Burle, Lancaster, PA) attached to the microscope. Images for the determination of individual cell motility were recorded from 10–12 different fields/well over a period of 15 or 20 min, with 1 or 2 min intervals, respectively.

### Determination of Cell Morphology and Single Cell Motility

For determinations of individual cell motility and morphology contours of live cells were recognised semi-automatically by means of thresholding and binary transformation of recorded images. This method allows determination of the centroid position and the calculation of various parameters of cell morphology, including average cell brightness, mean-cell-area, form factor and process domain. Form factor is defined mathematically as  $4\pi \times (\text{mean-cell-area})/(\text{cell perimeter})^2$ . Thus, a perfectly round cell will have a form factor of 1, whereas more elongated or stellate cells will have a lower form factor. The process domain is defined as the area obtained by subtracting the object area from the convex hull area. Thus, the process domain increases with increasing number and length of processes [Soll et al., 1988; Kawa et al., 1998].

Calculations of cell motility were based on determinations of the centroid positions of individual cells or, alternatively, by manual marking of the centre of the nuclei of individual cells. Centroids or nuclear centres from consecutive video frames were utilised for the determination of the mean cellular displacement,  $\tau$ , of individual cells. Subsequently, cellular motility was determined as the mean-cell-speed,  $S_\tau = \langle d \rangle / \tau$  using overlapping intervals for the calculations, and a time interval,  $\langle d \rangle$ , of 10 min [Dunn, 1983; Stokes et al., 1991; Walmod et al., 1998]. In order to exclude the influence of

cell-cell interactions on cellular motility and morphology, only single cells were evaluated.

### Immunofluorescence Microscopy

Cells were seeded on four well plastic LabTek slides (Nunc) and grown as described above. When staining for  $\beta$ -tubulin, focal adhesion kinase (FAK), paxillin, phosphotyrosine and vinculin, cells were fixed in 3% (w/v) paraformaldehyde in PBS (10 min), permeabilized with 0.2% (v/v) Triton X-100 in PBS (2 min) and rinsed in PBS containing 1% BSA. Subsequently, they were incubated with either monoclonal antibodies against  $\beta$ -tubulin (Amersham, Hørsholm, Denmark) diluted 1:20 or monoclonal antibodies against FAK, Paxillin, phosphotyrosine (all from Transduction Laboratories, Lexington, KY) or vinculin (Sigma) diluted 1:25, followed by incubation with either a goat anti-mouse Ig-FITC conjugate (Calbiochem, La Jolla, CA) or a rabbit anti-mouse Ig-FITC conjugate (DAKO, Glostrup, Denmark). All dilutions were performed in PBS containing 10% goat or rabbit serum (depending on the species from which the secondary antibodies were obtained) and 0.05% Triton X-100.

For the visualisation of filamentous actin (F-actin) and gelsolin cells were rinsed in actin stabilising buffer (ASB; 10 mM Tris, 0.15 M NaCl, pH 7.4 containing 2 mM MgCl<sub>2</sub>, 0.2 mM dithioerythritol, 10% glycerol (v/v); [Knowles and McCulloch, 1992]), fixed in 3% paraformaldehyde in ASB (10 min), rinsed in ASB, permeabilized with 0.2% saponin in ASB (2 min) and stained using Texas Red X-conjugated phalloidin (Molecular Probes, Eugene, OR) diluted 1:30 in ASB, or rabbit antibodies against gelsolin (Chemicon, Temecula, CA) followed by incubation with a swine anti-rabbit Ig-rhodamin (DAKO, Denmark), both antibody solutions being diluted 1:25 in PBS containing 10% swine-serum and 0.05% Triton X-100.

Cells were mounted using Prolong Antifade (Molecular Probes) and scanned using a MultiProbe 2001 Laser Scanning Confocal Microscope equipped with an argon/krypton laser (Molecular Dynamics, USA) and a 60 $\times$  or 100 $\times$  objective (1.4 numerical aperture) (Nikon, Tokyo, Japan).

### Focal Adhesion Quantification

Immunofluorescence stainings of FAK, paxillin, phosphotyrosine and vinculin were performed as described above. Stainings of control cells and VPA-treated cells were performed on cells grown on the same multiwell slide (LabTek) using the same antibody solutions. From each staining several scanings were performed by confocal microscopy close to the cell-substratum interface using a 60 $\times$  objective and a 100 µm pinhole. All electronic settings were identical for scan-

nings of control and VPA-treated cells, respectively. Quantifications of cell areas and staining intensities were performed by manual drawing of cell outlines using the software "ImageSpace" version 3.2 (Molecular Dynamics). Average values of the background staining intensities for the individual stainings were subtracted from all measurements.

### F-Actin Quantification

Cells grown in 35 mm tissue culture dishes for 48 h were fixed and stained for F-actin as described above, and observed through a 20 $\times$  objective using a Nikon Diaphot 300 inverted microscope equipped with epifluorescence and a Nikon motorised shutter. 512  $\times$  512 pixel video images of stained cells were obtained using a black and white video camera with a BMK 800 operating unit (Grundig Electronic, Fürth, Germany) giving a linear correlation between the intensity of fluorescence of the sample and the grey level value in the corresponding recorded images. Average cell brightness was calculated as described previously [Berezin et al., 1996]. Under the chosen conditions no fading in fluorescence during recordings was observed.

### Cell Detachment Assay

Cells were plated in 96-well tissue culture plates (Nunc) at a concentration of  $7.5 \times 10^3$ – $1.25 \times 10^4$  cells/well and treated with VPA for varying times by adding VPA directly to the wells to a final concentration of 3 mM. Following incubation, the medium was removed from the wells, and cells were rinsed once in PBS (37°C), incubated with 0.5–4% (w/v) trypsin in PBS for 10 min (37°C, 5% CO<sub>2</sub>), rinsed twice in PBS, fixed in 3% (w/v) paraformaldehyde in PBS for 15 min and stained with 0.5% (w/v) crystal violet in 20% ethanol (v/v) for 15 min. Excess of crystal violet was removed by several rinses in milli-Q water, and finally the stain was solubilised in 0.1 M Na-citrate in 50 % ethanol, pH 4.2, overnight. Absorbance was measured at 550 nm using an ELISA-reader (SLT Labinstruments, Groedig, Austria).

### ATP-Induced Cell Contraction

Cells were plated in 35 mm culture dishes and grown as described above. Cell contraction induced by the addition of ATP to permeabilized cells was performed as described by Thoumine and Ott [1996]. Briefly, cells were rinsed once with rinsing buffer (RB; 10 mM Tris-HCl, 60 mM KCl, 125 mM sucrose, pH 7.0) at 4°C, permeabilized with Triton X-100 (0.005–0.120 % (v/v)) in RB (4°C, 10 min), rinsed once in RB (4°C) and incubated in contraction buffer (CB; 10 mM Tris-HCl, 30 mM KCl, 5 mM MgCl<sub>2</sub>, 3  $\mu$ M CaCl<sub>2</sub>, pH 7.0) with or without 100  $\mu$ M ATP (37°C, 10 min). Immediately following incubation in CB, phase-contrast images of

cells were acquired as described above. Alternatively, cells were incubated in the presence or absence of 100  $\mu$ M ADP, or pretreated with 1  $\mu$ g/ml cytochalasin D for 50 min prior to initiation of ATP-induced contraction. Images of contracted cells were processed for the determination of cellular morphology as described above.

### Statistics and Graphical Presentations

Statistics and graphical presentations were performed using PRIMA (Protein Laboratory, Copenhagen, Denmark) and "Fig. P" v2.2 (Biosoft, Cambridge, UK). Statistical evaluations were performed using a two-sided Student's *t*-test. Unless stated otherwise the results are given as mean  $\pm$  SEM calculated on the basis of cell number.

## RESULTS

### Long-Term Exposure to VPA Modulates Cellular Morphology Through Alterations in Cytoskeletal Organisation

VPA has previously been demonstrated to cause dose- and time-dependent changes in cell morphology, the most prominent being a pronounced increase in cell area [Berezin et al., 1996]. In order to study the contribution of cytoskeletal elements to the morphology of L-cells treated with VPA, experiments were performed in which microtubules and actin filaments were disrupted with nocodazole and cytochalasin D, respectively. Cells were grown for 48 h in the absence or presence of 3 mM VPA followed by a 50 min incubation in 10  $\mu$ g/ml nocodazole or 1  $\mu$ g/ml cytochalasin D.

VPA treatment caused an increased spreading and flattening of the cells (Fig. 1b, f) when compared to control cells (Fig. 1a, e) and a changed distribution of F-actin as reflected by an increased amount of stress fibres, and a decrease in cortical F-actin and in the amount of membrane ruffles (Fig. 1f vs. e). In contrast, no significant change in the organisation of microtubules was apparent (Fig. 1b vs. a).

Exposure to nocodazole caused an almost total disintegration of microtubules (Fig. 1c, d). Likewise, exposure to cytochalasin D caused a complete collapse of the microfilament cytoskeleton, leaving the F-actin in large aggregates within the cells (Fig. 1g, h). Figure 2 summarises the quantitative effects of the various treatments on cellular morphology. VPA induced a significant increase in mean-cell-area and process domain, and a significant decrease in form factor when compared to control cells, showing that VPA caused the cells to become larger and acquire more and/or longer processes. Treatment with nocodazole caused both control cells and VPA-treated cells to round up as reflected by a statistically significant decrease in mean-cell-area and process

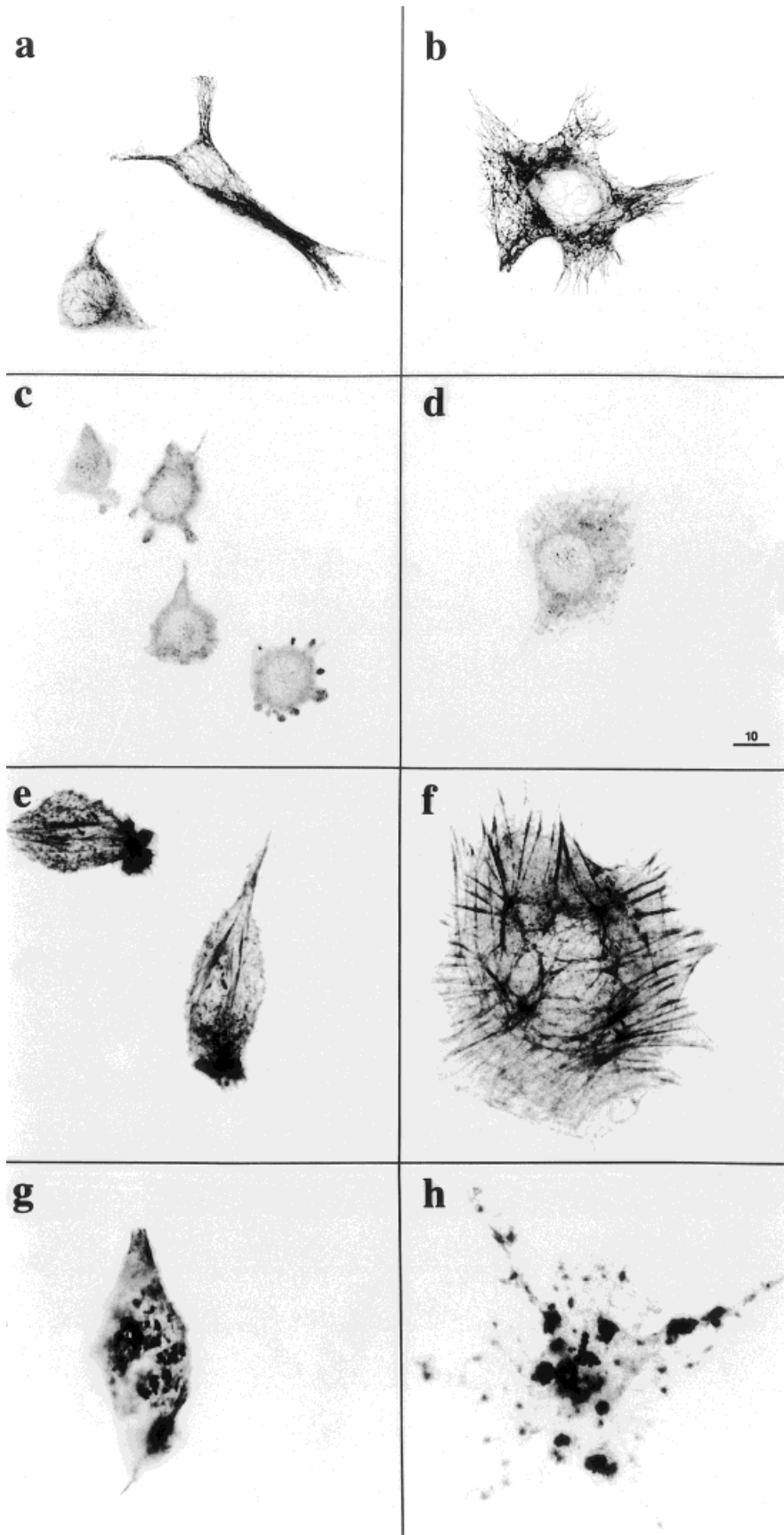


Fig. 1. Inverted fluorescence micrographs of  $\beta$ -tubulin (a, b, c, d) and F-actin (e, f, g, h). L-cells were grown for 48 h in the absence (a, c, e, g) or presence (b, d, f, h) of 3 mM VPA. Cells in c and d were pre-treated with nocodazole. Cells in g and h were pre-treated with cytochalasin D. Micrographs e and f are three-dimensional images composed of section series using a stepsize of 0.30  $\mu$ m. Other images are single section scanings taken close to the cell-substratum interface. Bars indicate dimensions in  $\mu$ m.

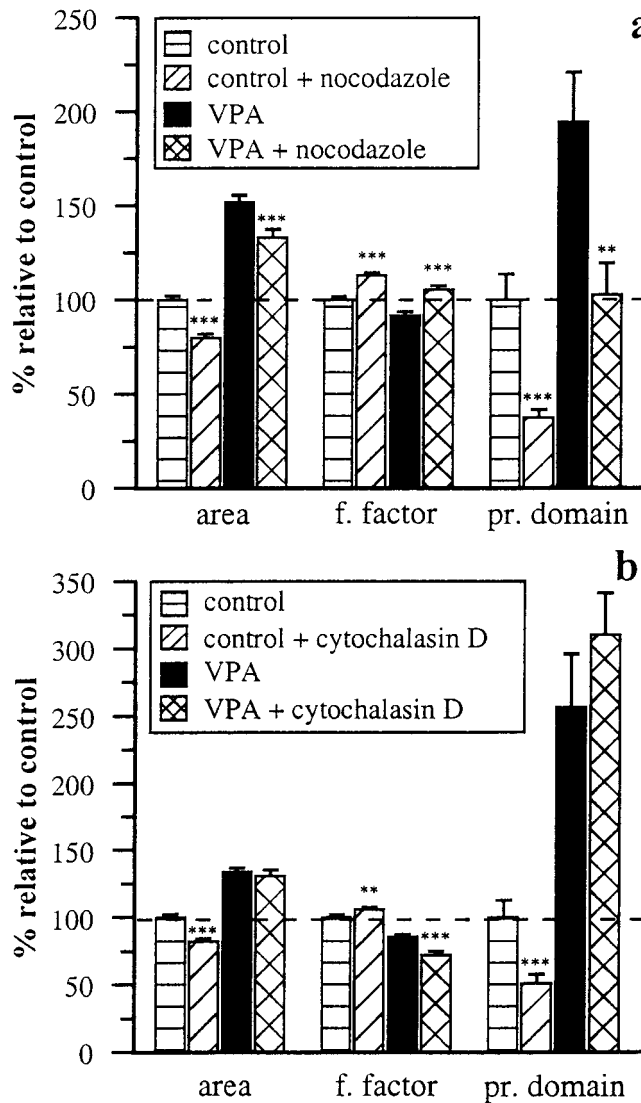


Fig. 2. Quantitative determinations of mean-cell-area, form factor and process domain of L-cells grown for 48 h in the absence or presence of 3 mM VPA and pre-treated without or with nocodazole (a) or cytochalasin D (b). Values are normalised in relation to control cells. The number of cells in the individual experiments was in the range of 147–453. \*\*\* $P < 0.001$ , \*\* $P < 0.005$  (nocodazole and cytochalasin D-treated cells vs. untreated cells). All values for VPA-treated cells not treated with nocodazole or cytochalasin D were significantly different from values for untreated control cells ( $P < 0.005$  or lower).

domain, and a statistically significant increase in form factor (Fig. 2a). Thus, the morphology of both control cells and VPA-treated cells was dependent on an intact tubulin cytoskeleton, and the increased amount of stress-fibres in VPA-treated cells did not seem to reduce the requirement of these cells for intact microtubules for maintenance of cell morphology.

Treatment with cytochalasin D affected control cells and VPA-treated cells differently. Control cells

responded to cytochalasin D treatment by rounding up. In contrast, VPA-treated cells exposed to cytochalasin D exhibited no significant change in mean-cell-area, but a statistically significant decrease in form factor, indicating an increase in process length or process number. In agreement with these data, the majority of VPA-treated cells exposed to cytochalasin D acquired a starlike phenotype (Fig. 1h). Thus, although VPA treatment only seems to cause visible alterations in the F-actin cytoskeleton the morphology of VPA-treated cells were less sensitive to disruption of the actin cytoskeleton with cytochalasin D than the morphology of control cells. This indicates that the morphology of VPA-treated cells is more dependent on intact microtubules than the morphology of control cells.

### Long-Term Exposure to VPA Causes an Increase in the Concentration of F-Actin

In order to clarify, whether the observed changes in the organisation of the actin filaments in VPA-treated cells were a result of redistribution of F-actin, or whether it resulted from changes in the amount of F-actin, a quantitative determination of the cellular amount of F-actin was performed. Following incubation for 48 h in the absence or presence of 3 mM VPA, F-actin content was quantified on the basis of video images of phalloidin stained cells. Control cells were shown to have a 34% higher amount of F-actin per area unit than VPA-treated cells. However, the volume of VPA-treated cells has previously been demonstrated not to be significantly different from untreated cells [Berezin et al., 1996]. Taking this into consideration, the relative amount of F-actin per cell was calculated and found to be statistically significantly higher by 23% in VPA-treated cells than in control cells. Thus, long-term exposure to VPA increased the cellular amount of F-actin.

### Long-Term Exposure to VPA Induces an Increased Cell-Substratum Adhesion

The motile behaviour of a cell has been shown to be modulated by the amount of focal adhesions and the expression of focal adhesion proteins [Ben-Ze'ev et al., 1994; Goldmann et al., 1995; Ilic et al., 1995]. As shown in Figure 3, cells treated with 3 mM VPA for 48 h (Fig. 3b) have more pronounced focal adhesions than control cells (Fig. 3a). In order to obtain a quantitative estimate of the alterations in focal adhesion formation immunofluorescence stainings of paxillin, vinculin, FAK, and phosphotyrosine were performed, and confocal images scanned close to the cell-substratum interface were acquired and quantified.

As shown in Figure 3c the mean staining intensity per cell was for all stainings significantly higher for VPA-treated cells than for control cells, indicating that

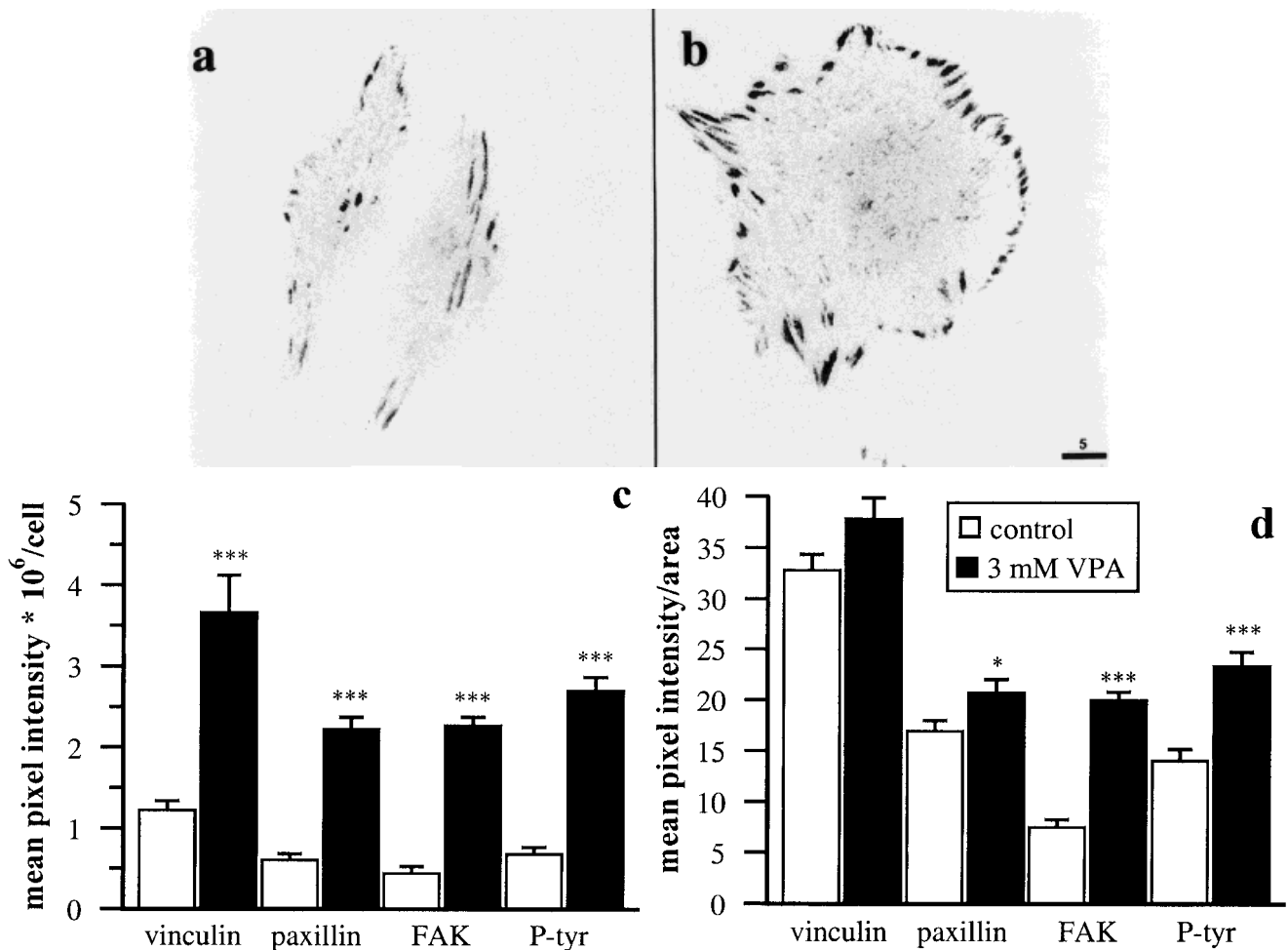


Fig. 3. **a, b:** Inverted confocal micrographs of vinculin in control cells (a) and cells treated with 3 mM VPA for 48 h (b). Bar indicates dimensions in  $\mu\text{m}$ . **c, d:** Quantitative estimation of the amount of selected focal adhesion markers located at the cell-substratum interface for control cells (white bars) and cells treated with 3 mM VPA for 48 h

(black bars). **c:** Mean intensity per cells. **d:** Mean intensity per area unit. The number of cells in the individual measurements of control cells and VPA-treated cells were 24 and 18 (vinculin), 7 and 20 (FAK), 50 and 38 (paxillin), and 15 and 13 (phosphotyrosine). \* $P < 0.05$ ; \*\* $P < 0.01$ ; \*\*\* $P < 0.001$ .

VPA-treatment caused a higher amount of focal adhesion proteins to be located at the ventral surface of the cells. Furthermore, the mean staining intensity per area unit of paxillin, FAK, and phosphotyrosine was statistically significantly higher in VPA-treated than in control cells, and the same trend was seen for vinculin (Fig. 3d).

The increased focal adhesion formation in VPA-treated cells supported the suggestion that VPA might cause a decrease in cell motility through increased cell-substratum adhesion. To test this possibility a cell detachment assay was performed. Cells grown in the absence or presence of VPA for varying times were treated with varying concentrations of trypsin, and the cells remaining after subsequent washings in PBS were fixed, stained, and quantified.

Figure 4 shows data from a representative experiment. Untreated cells, or cells exposed to VPA for 1, 4 or

24 h all seemed to be detached from the substratum at identical trypsin concentrations. However, cells exposed to VPA for 48 h were significantly more strongly attached than control cells, as seen by the increased proportion of cells remaining attached following trypsin treatment. When determining the  $\text{IC}_{50}$  values of trypsin for detachment, it was found that 48 h treatment with VPA increased the  $\text{IC}_{50}$  value for inhibition of attachment by more than 100% when compared to the  $\text{IC}_{50}$  value for control cells (Fig. 4, insert). Thus, long-term exposure to VPA caused an increased attachment of L-cells to the substratum.

#### Exposure of VPA-Treated Cells to an RGD-Containing Peptide Only Partially Rescues the Inhibition of Their Motile Behaviour

In order to test whether the observed increase in cell-substratum attachment was responsible for the ob-

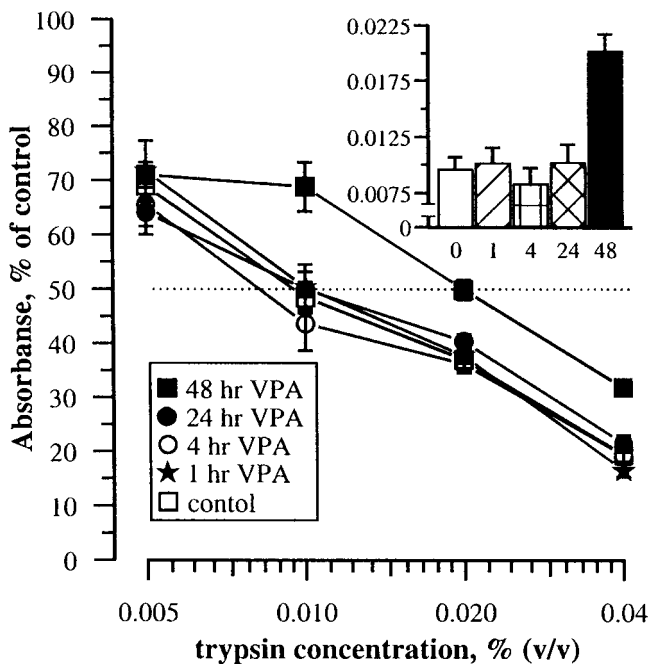


Fig. 4. Trypsin cell-detachment assay. 48-hour cultures of L-cells seeded in 96-well culture plates were exposed to trypsin in PBS, rinsed, fixed, stained with crystal violet, and quantified using an ELISA reader. Cells remaining after trypsinisation are expressed in % of the amount of cells in wells incubated with PBS in the absence of trypsin. Each determination is based on the measurements of eight individual wells. The **insert** shows  $IC_{50}$ -values of the trypsin concentration for detachment after varying times of VPA-treatment. Bars indicate mean  $\pm$  SEM.

served changes in cellular morphology and motility of VPA-treated cells, cell morphology and motility was monitored after incubation with an RGD-containing peptide which is known to cause decreased cell-substratum attachment by competing with the binding of integrins to RGD-expressing components of the extracellular matrix [Pierschbacher and Ruoslahti, 1984].

Exposure to 100  $\mu$ g/ml RGD caused both control cells and VPA-treated cells to round up (Fig. 5b, d vs. a, c). However, from quantitative estimations it appeared, that whereas control cells responded strongly to RGD treatment as reflected by a significant 17% increase in form factor and a significant 71% decrease in process domain, VPA-treated cells were more resistant to the treatment exhibiting only a 13% increase in form factor, and no significant change in process domain (data not shown).

Short-term recordings of cell motility showed that mean-cell-speed of VPA-treated cells increased in response to RGD treatment, however, not up to the level of untreated control cells (Fig. 6). Thus, RGD treatment was only capable of a partial rescue of the VPA-induced reduction in cellular motility, indicating that the increased

attachment caused by the drug did contribute to, but was not the sole cause of the decreased motility.

### VPA Does Not Affect the Contractile Abilities of the Actomyosin Cytoskeleton

As the increased cell-substratum attachment of VPA-treated cells only partially accounted for the reduced cellular motility, the main reason for the changed motile behaviour might be ascribed to alterations in the dynamics of the actin cytoskeleton. As one of the requirements for cell motility is the ability of the actomyosin complex to contract in order to cause translocation of the cell body, it was investigated whether VPA interfered directly with this process. To test this possibility, an analysis of ATP-induced contraction of actomyosin complexes in permeabilized cells was performed according to Thoumine and Ott [1996].

Based on changes in the cellular form factor the optimal concentration of Triton X-100 for permeabilization was determined to be 0.02% (v/v) (Fig. 7). It can be seen that both control cells and VPA-treated cell were capable of contraction upon incubation with ATP, leading to an increase in form factor. Interestingly, VPA-treated cells responded more strongly to ATP than did control cells, the relative increase in form factor being 75 and 35%, respectively. Comparable results were obtained for the mean-cell-area, for which a relative decrease of 30 and 20% was observed for VPA-treated cells and control cells, respectively (data not shown). Incubation in the presence of ADP did not cause a change in form factor, indicating that the induced contraction was caused specifically by ATP. Furthermore, preincubation with cytochalasin D left the cells unable to respond to ATP, indicating that it was indeed actomyosin that was responsible for the observed contraction (data not shown).

These results demonstrate, that both control cells and cells treated with VPA seemed to possess actomyosin complexes capable of contraction. Therefore, the inhibition of cellular motility induced by VPA cannot be explained by an inability of actomyosin to facilitate cell body translocation.

### VPA Causes a Redistribution of Gelsolin, and Inhibits the Effect of a $PIP_2$ Binding Gelsolin Fragment

As the contractile abilities of actomyosin complexes seemed to be intact in VPA-treated cells, we investigated whether VPA affected the dynamic regulation of F-actin assembly and disassembly. One of the key proteins involved in F-actin dynamics is gelsolin, and therefore the distribution of gelsolin in control cells and VPA-treated cells was investigated. From Figure 8 it can be seen that VPA treatment caused a redistribution of gelsolin in cells. In control cells the protein was mainly

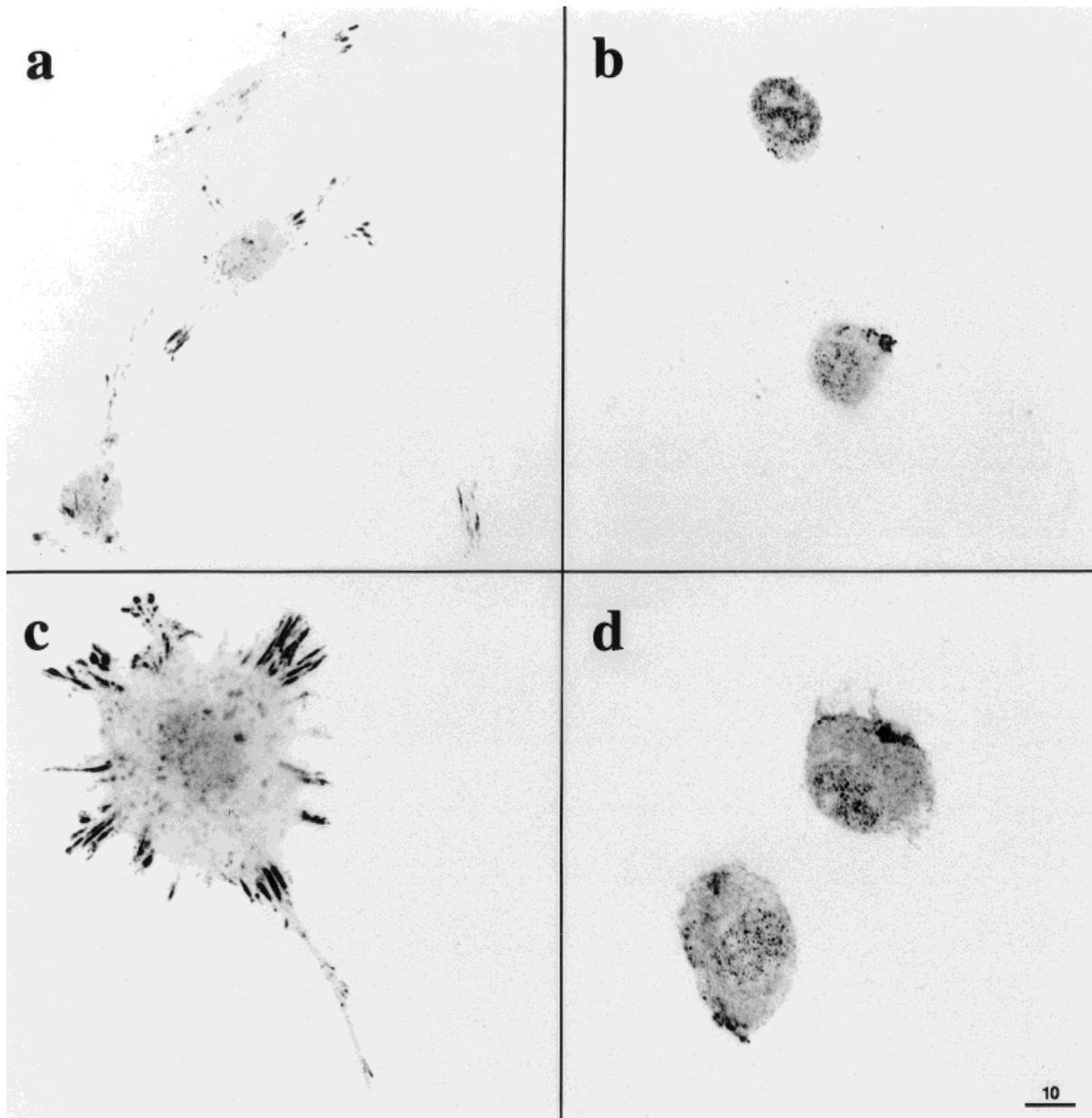


Fig. 5. Inverted confocal micrographs showing immunofluorescence stainings of FAK. L-cells were grown for 48 h and pre-treated without or with an RGD-containing peptide (100  $\mu\text{g}/\text{ml}$ ). **a**, control; **b**, control + RGD; **c**, 3 mM VPA; **d**, 3 mM VPA + RGD. Micrographs show single section scanings taken close to the cell-substratum interface. Bar indicates dimensions in  $\mu\text{m}$ .

localised in peripheral membrane ruffles (Fig. 8a), whereas gelsolin in VPA-treated cells exhibited a diffuse perinuclear localisation (Fig. 8b).

In order to test how cells responded to a modulation of gelsolin activity, 48-h cultures without or with 3 mM VPA treatment were incubated with a decapeptide containing one of the  $\text{PIP}_2$ -binding motifs of gelsolin. This peptide is known to enter live cells and to compete for gelsolin-binding to  $\text{PIP}_2$ , thereby leaving gelsolin in a

potential actin binding state (C.C. Cunningham, University of Florida, personal communication).

Figure 9 shows a time-response assay of the effect of two different concentrations of the gelsolin-peptide on the average cell brightness. Round, poorly attached cells exhibit a high brightness, and thus, this parameter is an indirect estimate of the degree of cell-substratum attachment and/or cell contraction. It is seen that control cells responded strongly and reversibly to the gelsolin-peptide

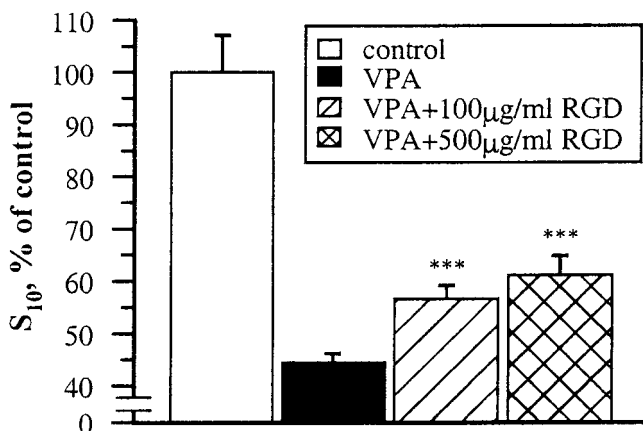


Fig. 6. Mean cell speed of 48-h cultures of L-cells untreated or treated with VPA following 50 min of exposure to 100 µg/ml or 500 µg/ml RGD. The presented data constitute a representative experiment. Values are normalised in relation to the speed of control cells. The number of cells in the individual measurements varied between 92 and 163. \*\*\* $P < 0.001$ .

in a dose-dependent manner (Fig. 9, open circles). 10 µM peptide caused a maximum response 1 h after addition, and cells returned to their original morphology within 2 h after treatment. 80 µM peptide caused a stronger and longer lasting response. In contrast, exposure of VPA-treated cells to the peptide caused insignificant changes in cell brightness (Fig. 9, solid circles). As shown in Figure 9 (insert) the exposure of 48-h cultures to 10 µM peptide caused a significant relative increase in the average brightness of control cells by 42%, whereas no significant increase could be demonstrated for VPA-treated cells. Similar results were obtained for the mean-cell-area, which decreased only in control cells upon treatment with the peptide (data not shown).

By fluorescence stainings of F-actin it could be seen, that the peptide caused control cells to round up, leaving the cells with fewer stress fibres. At the same time an increase in cortical actin was seen (Fig. 10c vs. a). In contrast, no significant changes in the cell morphology or distribution of F-actin could be identified in VPA-treated cells upon peptide exposure (Fig. 10d vs. b).

In conclusion, long-term exposure to VPA leads to a redistribution of gelsolin, leaving the protein in a state where it, in contrast to gelsolin in control cells, only responds insignificantly to the addition of the PIP<sub>2</sub>-binding gelsolin-peptide. Consequently, we suggest that the VPA-induced alteration in the gelsolin regulated dynamics of actin filaments contribute to the reduced motile behaviour and altered morphology of VPA-treated cells and, therefore, possibly to the teratogenic potential of the compound.

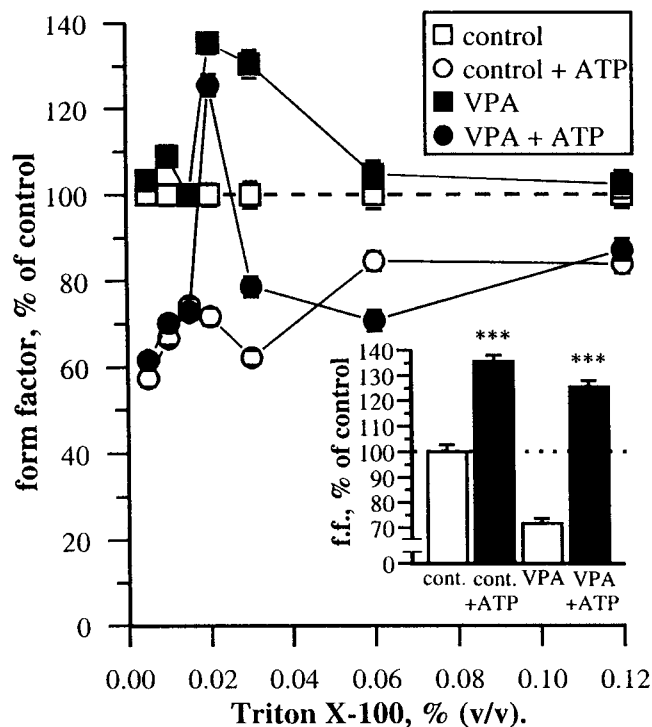


Fig. 7. ATP-induced cell contraction. 48-h cultures of L-cells treated without or with 3 mM VPA were permeabilized and incubated in the absence or presence of 100 µM ATP. Curves demonstrate the effect on form factor of ATP-induced contraction at various concentrations of Triton X-100. Results are at any given Triton X-100 concentration normalised to the form factor value of control cells not exposed to ATP. The individual data points are based on the morphological determination of approximately 250 single cells. The insert shows the effect of ATP-induced contraction on form factor for control and VPA-treated cells at 0.02 % Triton X-100. \*\*\* $P < 0.001$ .

## DISCUSSION

VPA is a widely used antiepileptic drug, which besides its anticonvulsive activity has been demonstrated to be teratogenic [Robert, 1988]. We have previously demonstrated that exposure to VPA and VPA analogues induce an increase in cell area and a decrease in cell motility in a manner correlating with the teratogenic potencies of the individual compounds [Berezin et al., 1996; Walmod et al., 1998]. In this study we have investigated possible alterations in the cytoskeleton of VPA-treated cells, which might account for these effects.

In accordance with previous observations long-term exposure of fibroblastoid L-cells to 3 mM VPA caused a significant change in cell morphology, resulting in an increase in the number and/or length of processes, mean-cell-area and the number of stress fibres, and a redistribution of F-actin.

Immunocytochemical stainings of β-tubulin did not reveal any changes in the concentration or organisation of microtubules as a result of the drug treatment. However, disruption of F-actin or microtubules with cytochalasin D

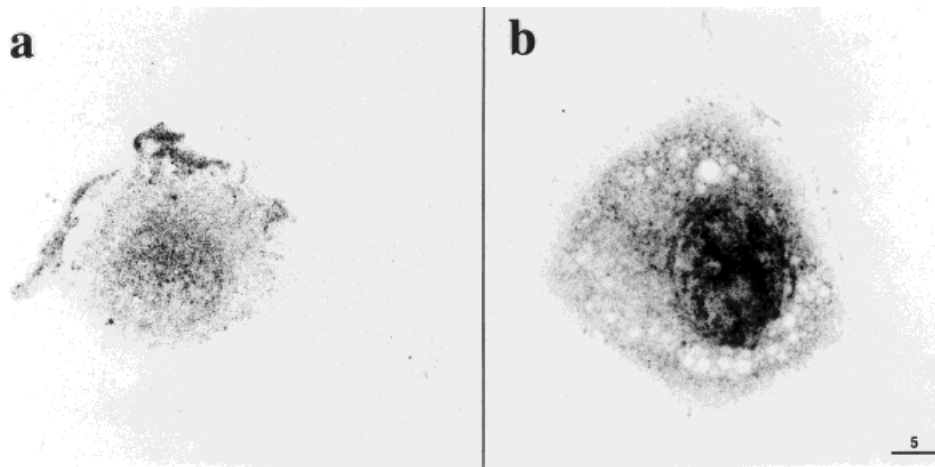


Fig. 8. Inverted confocal micrographs showing immunofluorescence stainings of gelsolin. L-cells grown for 48 h in the absence (a) or presence (b) of 3 mM VPA. Micrographs shown single section scanings taken close to the cell-substratum interface. Bar indicates dimensions in  $\mu\text{m}$ .

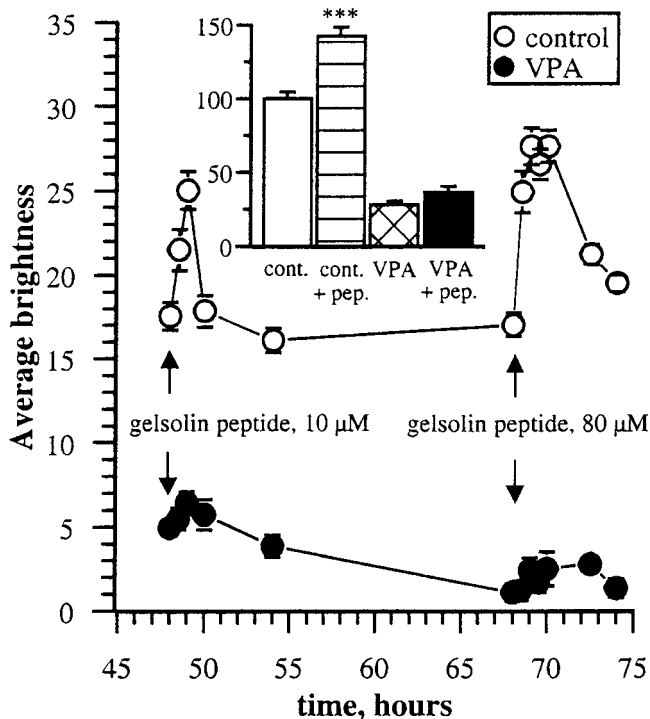


Fig. 9. Time- and dose-response of the effect of gelsolin-peptide treatment on average cell brightness. At the indicated times 10 or 80  $\mu\text{M}$  of a peptide containing the  $\text{PIP}_2$ -binding domain of gelsolin were added to the cultures. The individual data points are based on the morphological determination of 144–321 single cells. The insert demonstrates the effect on average cell brightness of exposure for 1 h to the gelsolin-peptide (10  $\mu\text{M}$ ). \*\*\* $P < 0.001$ .

and nocodazole, respectively, demonstrated that the altered morphology of VPA-treated cells was predominantly dependent on microtubules. Whereas disruption of F-actin in control cells caused cells to round up, VPA-treated cells reacted to the same treatment by adopting a

starlike shape with pronounced processes, which previously have been demonstrated to be rich in parallel bundles of microtubules [Berezin et al., 1997].

These observations might be explained based on the tensegrity model [reviewed Ingber et al., 1994] according to which the contractile forces generated by stress-fibres is counterbalanced by focal adhesions and microtubules acting as compression-resistant elements. Thus, the increased amount of stress-fibres in VPA-treated cells is expected to be counterbalanced by a reorganisation of microtubules.

In the present study it is also demonstrated that VPA treatment caused an increase in the amount of F-actin. However, whether this is caused by a general increase in actin expression or by alterations in the G/F-actin ratio has not been investigated. Previous studies—unrelated to investigations of VPA—have demonstrated that an increased amount of F-actin causes an increase in amount of vinculin and talin, and a larger proportion of vinculin in a Triton-insoluble state, indicating that the assembly state of actin regulates talin and vinculin by a feedback mechanism [Bershadsky et al., 1995; Schevzov et al., 1995]. Furthermore, cellular motility has been demonstrated to be inversely correlated to the cellular concentration of vinculin [Ben-Ze'ev et al., 1994; Goldmann et al., 1995]. Thus, the changes in cell motility and morphology observed upon long-term exposure to VPA might be an indirect consequence of the increased F-actin level affecting the amount and localisation of focal adhesion proteins. In agreement with this hypothesis long-term treatment with VPA was shown to cause more focal adhesion proteins to be directed towards focal adhesions, and to cause an increased cellular adhesion to the extracellular matrix. However, confocal Z-scans of stained cells demonstrated control cells to contain focal adhesion proteins

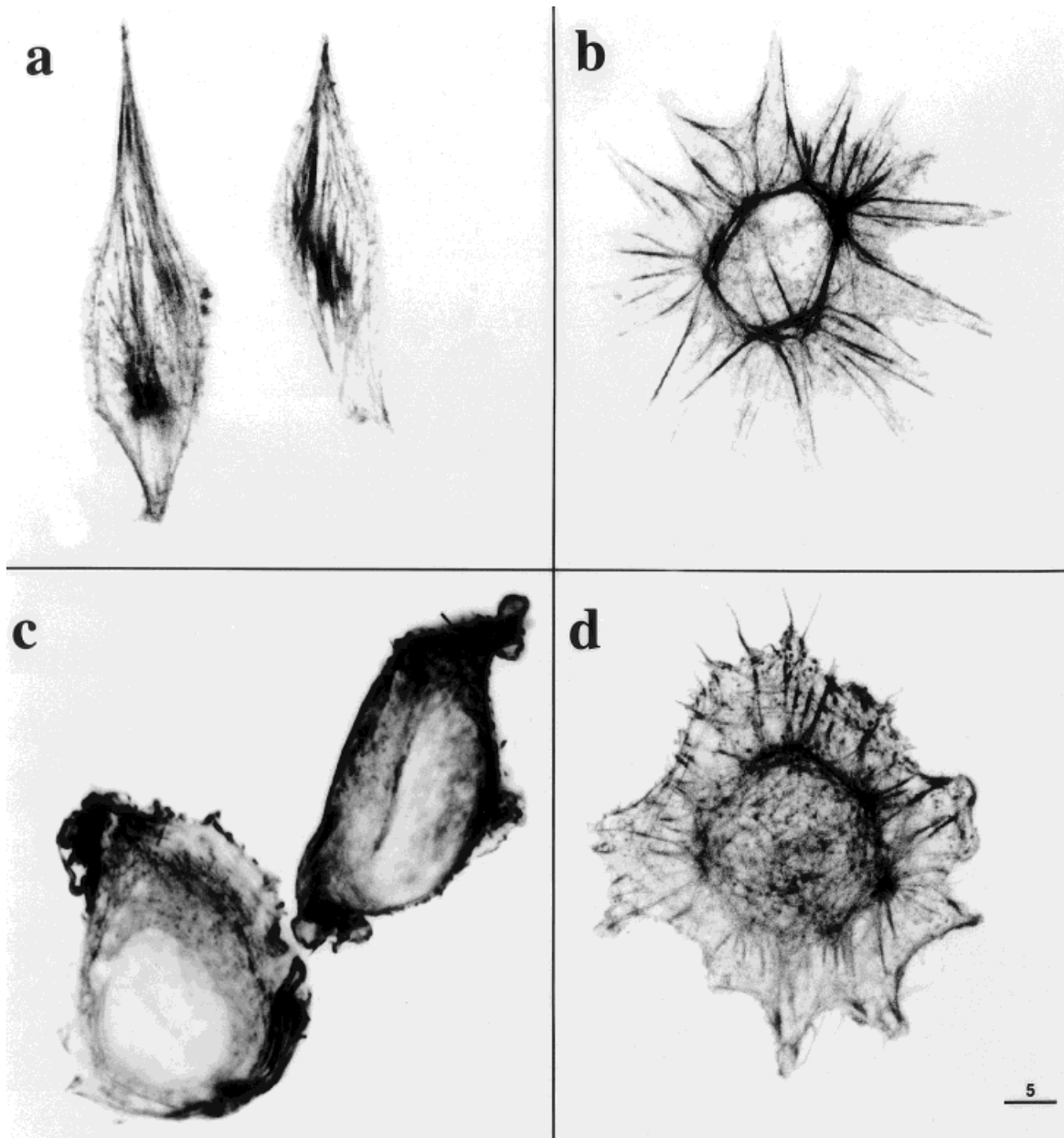


Fig. 10. Inverted confocal micrographs showing fluorescence stainings of F-actin. L-cells were grown for 48 h in the absence (a, c) or presence (b, d) of 3 mM VPA, followed by no treatment (a, b) or exposure for 1 h to 10  $\mu$ M gelsolin-peptide (c, d). Micrographs show scanings of single section taken close to the cell-substratum interface. Bar indicates dimensions in  $\mu$ m.

at the dorsal as well as the ventral surface, whereas these proteins almost exclusively were present at the ventral surface in VPA-treated cells (unpublished observation). Thus, the stronger staining of focal adhesions in VPA-treated cells most likely reflects a redistribution and not an increased expression of these proteins.

Cell adhesion is intimately involved in the formation of tissue architecture [reviewed by Gumbiner, 1996]. In vivo, individual cells are interconnected through the

so-called “extended cytoskeleton” created by intercellular junctions and transmembrane connections of the intracellular cytoskeleton with the ECM, and thus, changes in the balance of the intra- and intercellular forces, and in cell-substratum interactions cause morphological changes at the tissue level. For example, the induction of epithelial folding has been related to the relative adhesiveness of the cells [Nardi, 1981], and alterations in cellular adhesiveness have been suggested to be one of the factors

regulating neurulation [reviewed by Gordon, 1985]. Furthermore, mechanical stress has been shown to be a prerequisite for the invagination and bending of cell layers during gastrulation and neurulation [Belousov et al., 1975; Gordon and Brodland, 1987], and neurulation has been demonstrated to be inhibited by cytochalasin B-treatment [Karfunkel, 1972; Burnside, 1973]. Thus, from a mechanical point of view, the increased cellular adhesion and the increase in the amount of F-actin and stress fibres in VPA-treated cells may in itself contribute to the teratogenic effect of VPA by interfering with normal morphogenetic processes.

Interestingly, the increased attachment was not the sole cause of the decreased motility of VPA-treated cells, as a reduction in cell-substratum attachment achieved by incubation with an RGD-containing peptide did not return the motile behaviour of VPA-treated cells to a level comparable with that of the control cells, indicating that other factors also contributed to the decreased motility in these cells.

As contraction of the actomyosin cytoskeleton is a prerequisite for cell motility we investigated this phenomenon in permeabilized control cells and cells treated with VPA. Our experiments demonstrated that VPA-treated cells contained functional actomyosin complexes, and they even contracted relatively more strongly upon ATP-exposure than control cells. This is in accordance with the fact, that VPA-treated cells were found to contain more stress fibres and a higher amount of F-actin per cell than control cells. Thus, long-term exposure to VPA seemed to strengthen the actomyosin complexes, and the decrease in motility observed for VPA-treated cells did not seem to be caused by an inability of actomyosin to contract.

In addition to contraction, exposure of permeabilized fibroblasts to very high concentrations of ATP (5 mM) has been shown to cause an induction of tyrosine phosphorylation and a breakdown of focal adhesions [Crowley and Horwitz, 1995]. However, we observed no contraction of cells pretreated with cytochalasin D upon ATP addition and no effects of ADP addition, indicating that the contraction could be attributed to an ATP-dependent contraction of the actomyosin cytoskeleton, and not to e.g. disassembly of focal adhesions.

Gelsolin is a protein known to be involved in nucleation, severing and capping of actin filaments in eukaryotic cells [Burtinck et al., 1997]. Reports concerning the role of gelsolin in cell motility are contradictory. Overexpression of gelsolin has been found to increase cellular motility [Cunningham et al., 1991], whereas fibroblasts derived from gelsolin null-mice exhibit a decreased cellular motility [Witke et al., 1995]. Other studies have demonstrated that the effect of gelsolin on cell motility is determined by a  $\text{Ca}^{2+}$ -dependent activa-

tion of the protein rather than its actual concentration [Arora and McCulloch, 1996; Cooper et al., 1987].

In the present study VPA was demonstrated to cause a redistribution of gelsolin from a peripheral localisation in membrane ruffles to a diffuse perinuclear location. In order to determine whether this altered distribution was accompanied by a change in gelsolin activity, we tried to modulate the amount of free gelsolin in living cells by incubating these with a peptide corresponding to a  $\text{PIP}_2$ -binding motif of gelsolin (residue 161–172) [Burtinck et al., 1997; Janmey et al., 1992]. This procedure is a relatively crude way of activating gelsolin, as it might also modulate the activity of other  $\text{PIP}_2$ -binding proteins (e.g. villin, vinculin and phospholipases). The treatment caused pronounced dose-dependent morphological changes in control cells including a rearrangement of F-actin, but not in VPA-treated cells. Transfection leading to expression of the same peptide in NR6 cells has previously been reported to cause an increase in the basal cell motility of these cells by dissociating gelsolin from the plasma membrane [Chen et al., 1996]. However, no consistent alterations in the motility of either control cells or VPA-treated cells was seen upon exposure to the gelsolin-peptide (unpublished observations).

Platelets and fibroblasts from gelsolin null-mice have been demonstrated to possess increased levels of F-actin [Barkalow et al., 1996; Witke et al., 1995], and dermal fibroblasts from gelsolin null-mice contain more stress fibres, have a larger mean-cell-area, and increased contractile capabilities [Witke et al., 1995]. Thus, the behaviour of cells derived from gelsolin null-mice seems to mimic the observed behaviour of VPA-treated cells, supporting the view that an altered activity of gelsolin leading to changes in the dynamics of the actin cytoskeleton might partially explain the observed VPA-induced changes in cell morphology and motility.

The demonstrated effects of VPA all required long-term exposure (48 h) to the drug, indicating that gelsolin probably is not the primary target of VPA. Besides the observed effects on cellular motility and morphology, VPA has also been demonstrated to arrest cells in the G1 phase of the cell cycle [Martin and Regan, 1991]. These effects point towards an VPA-induced alteration in signalling e.g. through the mitogen-activated protein (MAP) kinase pathway. Interestingly, cell motility has recently been demonstrated to be regulated by the MAP-kinase pathway, the kinases ERK1 and ERK2 enhancing myosin light chain kinase activity and the subsequent phosphorylation of myosin light chain [Klemke et al., 1997]. Whether the MAP-kinase pathway is affected by VPA is currently unknown, since the primary target(s) for VPA remain to be determined.

## REFERENCES

- Albrecht-Buehler G. 1987. Role of cortical tension in fibroblast shape and movement. *Cell Motil Cytoskeleton* 7:54–67.
- Andrews JE, Ebron-McCoy M, Bojic U, Nau H, Kavlock RJ. 1995. Validation of an in vitro teratology system using chiral substances: stereoselective teratogenicity of 4-en-valproic acid in cultured mouse embryos. *Toxicol Appl Pharmacol* 132:310–316.
- Andrews JE, Ebron-McCoy MT, Bojic U, Nau H, Kavlock RJ. 1997. Stereoselective dysmorphogenicity of the enantiomers of the valproic acid analogue 2-N-propyl-4-pentynoic acid (4-yn-VPA): cross-species evaluation in whole embryo culture. *Teratology* 55:314–318.
- Arora PD, McCulloch CAG. 1996. Dependence of fibroblast migration on actin severing activity of gelsolin. *J Biol Chem* 271:20516–20523.
- Barkalow K, Witke W, Kwiatkowski DJ, Hartwig JH. 1996. Coordinated regulation of platelet actin filament barbed ends by gelsolin and capping protein. *J Cell Biol* 134:389–399.
- Belousov LV, Dorfman JG, Cherdantzev VG. 1975. Mechanical stresses and morphological patterns in amphibian embryos. *J Embryol Exp Morphol* 34:559–574.
- Ben-Ze'ev A, Fernández JLR, Glück U, Salomon D, Geiger B. 1994. Changes in adhesion plaque protein levels regulate cell motility and tumorigenicity. In: Estes JE, Higgins PJ, editors. *Actin: biophysics, biochemistry, and cell biology*. New York: Plenum Press, p 147–157.
- Berezin V, Kawa A, Bojic U, Foley A, Nau N, Regan C, Edvardsen K, Bock E. 1996. Teratogenic Potency of Valproate Analogues evaluated by Quantitative Estimation of Cellular Morphology in vitro. *Toxicol In Vitro* 10:585–594.
- Berezin V, Walmod PS, Kawa A, Bock E. 1997. The anticonvulsive drug VPA affects cell morphology and cytoskeletal organization. In: Teelken A, Korf J, editors. *Neurochemistry: cellular, molecular, and clinical aspects*. New York: Plenum Press, p 295–298.
- Bershadsky AD, Glück U, Denisenko ON, Sklyarova TV, Spector I, Ben-Ze'ev A. 1995. The state of actin assembly regulates actin and vinculin expression by a feedback loop. *J Cell Sci* 108:1183–1193.
- Bowden CL, Brugger AM, Swenn AA, Calabrese JR, Janicak PG, Petty F, Dilsaver SC, Davis JM, Rush AJ, Small JG. 1994. Efficacy of divalproex vs lithium and placebo in the treatment of mania. *JAMA* 271:918–924.
- Bronner-Fraser M. 1993. Neural crest cell migration in the developing embryo. *Trends Cell Biol* 3:392–397.
- Burnside B. 1973. Microfilaments and microtubules in newt neurotation. *Am Zool* 13:989–1006.
- Burtneck LD, Koepf EK, Grimes J, Jones Y, Stuart DI, McLaughlin PJ, Robinson RC. 1997. The crystal structure of plasma gelsolin: implications for actin severing, capping, and nucleation. *Cell* 90:661–670.
- Chen P, Murphy-Ullrich JE, Wells A. 1996. A role for gelsolin in actuating epidermal growth factor receptor-mediated cell motility. *J Cell Biol* 134:689–698.
- Cooper JA, Bryan J, Schwab III B, Frieden C, Loftus DJ, Elson EL. 1987. Microinjection of gelsolin into living cells. *J Cell Biol* 104:491–501.
- Crowley E, Horwitz AF. 1995. Tyrosine phosphorylation and cytoskeletal tension regulate the release of fibroblast adhesion. *J Cell Biol* 131:525–537.
- Cunningham CC, Stossel TP, Kwiatkowski DJ. 1991. Enhanced motility in NIH 3T3 fibroblasts that overexpress gelsolin. *Science* 251:1233–1236.
- Domina LV, Rovensky JA, Vasiliev JM, Gelfand IM. 1985. Effect of microtubule-destroying drugs on the spreading and shape of cultured epithelial cells. *J Cell Sci* 74:267–282.
- Dunn GA. 1983. Characterising a kinesis response: time averaged measures of cell speed and directional persistence. In: Keller H, Till GO, Arbor A, editors. *Leukocyte locomotion and chemotaxis*. Basel, Boston, Stuttgart: Birkhäuser Verlag, p 14–33.
- Fisher JE Jr, Acuff-Smith KD, Schilling MA, Nau H, Vorhees CV. 1994. Trans-2-ene-valproic acid is less behaviorally teratogenic than an equivalent dose of valproic acid in rats. *Teratology* 49:479–486.
- Gail MH, Boone CW. 1972. Cell-substrate adhesivity: a determinant of cell motility. *Exp Cell Res* 70:33–40.
- Goldmann WH, Schindl M, Cardozo TJ, Ezzell RM. 1995. Motility of vinculin-deficient F9 embryonic carcinoma cells analyzed by video, laser confocal, and reflection interference contrast microscopy. *Exp Cell Res* 221:311–319.
- Gordon R. 1985. A review of the theories of vertebrate neurulation and their relationship to the mechanics of neural tube birth defects. *J Embryol Exp Morphol* 89(Suppl):229–255.
- Gordon R, Brodland GW. 1987. The cytoskeletal mechanics of brain morphogenesis: cell state splitters cause primary neural induction. *Cell Biophys* 11:177–238.
- Gumbiner BM. 1996. Cell adhesion: the molecular basis of tissue architecture and morphogenesis. *Cell* 84:345–357.
- Gunning P, Leavitt J, Muscat G, Ng S-Y, Kedes L. 1987. A human  $\beta$ -actin expression vector system directs high-level accumulation of antisense transcripts. *Proc Natl Acad Sci USA* 84:4831–4835.
- Hauzenberger D, Klominek J, Holgersson J, Bergstrom SE, Sundqvist KG. 1997. Triggering of motile behavior in T lymphocytes via cross-linking of alpha 4 beta 1 and alpha L beta 2. *J Immunol* 158:76–84.
- Ilic D, Furuta Y, Kanazawa S, Takeda N, Sobue K, Nakatsuji N, Nomura S, Fujimoto J, Okada M, Yamamoto T. 1995. Reduced cell motility and enhanced focal adhesion contact formation in cells from FAK-deficient mice. *Nature* 377:539–544.
- Ingber DE, Dike L, Hansen L, Karp S, Liley H, Maniotis A, McNamee H, Mooney D, Plopper G, Sims J, Wang N. 1994. Cellular tensegrity: exploring how mechanical changes in the cytoskeleton regulate cell growth, migration, and tissue pattern during morphogenesis. *Int Rev Cytol* 150:173–224.
- Janmey PA, Lamb J, Allen PG, Matsudaira PT. 1992. Phosphoinositide-binding peptides derived from the sequences of gelsolin and villin. *J Biol Chem* 267:11818–11823.
- Karfunkel P. 1972. The activity of microtubules and microfilaments in neurotation in the chick. *J Exp Zool* 181:289–302.
- Kawa A, Stahlhut M, Berezin A, Bock E, Berezi, V. 1998. A simple procedure for morphometric analysis of processes and growth cones of neurons in culture using parameters derived from the contour and convex hull of the object. *J Neurosci Methods* 79:53–64.
- Kislauskis EH, Zhu X-c, Singer RH. 1997.  $\beta$ -actin messenger RNA localization and protein synthesis augment cell motility. *J Cell Biol* 136:1263–1270.
- Klemke RL, Cai S, Giannini AL, Gallagher PJ, de Lanerolle P, Cheresch DA. 1997. Regulation of cell motility by mitogen-activated protein kinase. *J Cell Biol* 137:481–492.
- Knowles GC, McCulloch CAG. 1992. Simultaneous localization and quantification of relative G and F actin content: optimization of fluorescence labeling methods. *J Histochem Cytochem* 40:1605–1612.
- Maguire C, Regan CM. 1991. In vitro screening for anticonvulsant-induced teratogenesis: drug alteration of cell adhesivity. *Int J Dev Neurosci* 9:581–586.

- Martin ML, Regan CM. 1991. The anticonvulsant valproate teratogen restricts the glial cell cycle at a defined point in the mid-G1 phase. *Brain Res* 554:223–228.
- Martin ML, Breen KC, Regan CM. 1988. Perturbations of cellular function integral to neural tube formation by the putative teratogen sodium valproate. *Toxicol In Vitro* 2:43–48.
- Mattson RH. 1995. Efficacy and adverse effects of established and new antiepileptic drugs. *Epilepsia* 36(Suppl 2):S13–S26.
- McCawley LJ, O'Brien P, Hudson LG. 1997. Overexpression of the epidermal growth factor receptor contributes to enhanced ligand-mediated motility in keratinocyte cell lines. *Endocrinology* 138:121–127.
- Meyer MB, Bastholm L, Nielsen MH, Elling F, Rygaard J, Chen W, Öbrink B, Bock E, Edvardsen K. 1995. Localization of NCAM on NCAM-B-expressing cells with inhibited migration in collagen. *APMIS* 103:197–208.
- Nardi JB. 1981. Epithelial invagination: adhesive properties of cells can govern position and directionality of epithelial folding. *Differentiation* 20:97–103.
- Palecek SP, Loftus JC, Ginsberg MH, Lauffenburger DA, Horwitz AF. 1997. Integrin-ligand binding properties govern cell migration speed through cell-substratum adhesiveness. *Nature* 385:537–540.
- Pierschbacher MD, Ruoslahti E. 1984. Cell attachment activity of fibronectin can be duplicated by small synthetic fragments of the molecule. *Nature* 309:30–33.
- Robert E. 1988. Valproic acid as a human teratogen. *Congenital Anom* 28 (Suppl):S71–S80.
- Rønnov-Jessen L, Petersen OW. 1996. A function for filamentous  $\alpha$ -smooth muscle actin: retardation of motility in fibroblasts. *J Cell Biol* 134:67–80.
- Schevzov G, Lloyd C, Gunning P. 1995. Impact of altered actin gene expression on vinculin, talin, cell spreading and motility. *DNA Cell Biol* 14:689–700.
- Soll DR, Voss E, Varnum-Finney B, Wessels D. 1988. "Dynamic morphology system": a method for quantitating changes in shape, pseudopod formation, and motion in normal and mutant amoebae of *Dictyostelium discoideum*. *J Cell Biochem* 37:177–192.
- Sørensen KV. 1988. Valproate: a new drug in migraine prophylaxis. *Acta Neurol Scand* 78:346–348.
- Stokes CL, Lauffenburger DA, Williams SK. 1991. Migration of individual microvessel endothelial cells: stochastic model and parameter measurement. *J Cell Sci* 99:419–430.
- Thoumine O, Ott A. 1996. Influence of adhesion and cytoskeletal integrity on fibroblast traction. *Cell Motil Cytoskeleton* 35:269–280.
- Van Roy F, Mareel M. 1992. Tumour invasion: effects of cell adhesion and motility. *Trends Cell Biol* 2:163–169.
- Walmod PS, Foley A, Berezin A, Ellerbeck U, Nau H, Bock E, Berezin V. 1998. Cell motility is inhibited by valproic acid and its teratogenic analogues. *Cell Motil Cytoskeleton* 40:220–237.
- Willingham MC, Yamada KM, Yamada SS, Pouysségur J, and Pastan I. 1977. Microfilament bundles and cell shape are related to adhesiveness to substratum and are dissociable from growth control in cultured fibroblasts. *Cell* 10:375–380.
- Witke W, Sharpe AH, Hartwig JH, Azuma T, Stossel TP, Kwiatkowski DJ. 1995. Hemostatic, inflammatory, and fibroblast responses are blunted in mice lacking gelsolin. *Cell* 81:41–51.